Morphing of Image Represented Objects Using a Physical Methodology

Raquel Ramos Pinho
LOME – Laboratório de Óptica e Mecânica Experimental
Rua Dr. Roberto Frias, s/n
4200-465 OPORTO
PORTUGAL
rpinho@fe.up.pt

João Manuel R. S. Tavares
LOME, FEUP – Faculdade de Engenharia da Universidade do Porto
Rua Dr. Roberto Frias, s/n
4200-465 OPORTO
PORTUGAL
tavares@fe.up.pt

ABSTRACT

This paper presents a methodology to do morphing between image represented objects, attending to their physical properties. It can be used amongst images of different objects, or otherwise, between different images of the same object.

According to the used methodology the given objects are modelled by the Finite Element Method, and some nodes are matched by Modal Analysis. Then, by solving the Dynamic Equilibrium Equation the displacement field is determined, which allows the simulation of the objects' deformation.

This physical approach also allows the computation of the involved strain energy, therefore the estimated morphing can be represented by the local or global strain energy values.

This paper also describes the solution used to simulate only the non-rigid components of the involved deformation.

Categories and Subject Descriptors

I.2.10 [**Artificial Intelligence**]: Vision and Scene Understanding – *modeling and recovery of physical attributes, motion, shape.*

General Terms

Algorithms, Experimentation, Theory.

Keywords

Morphing, Deformable Objects, Dynamic Equilibrium Equation, Finite Element Method, Modal Analysis, Computer Vision.

1. INTRODUCTION

Although much has been done in 2D objects' morphing, the obtained results are not always coherent with the physical properties of the represented objects, and/or with the charges applied on them. These demands of some domains, like computer vision, computer graphics or medical image, can be satisfied through the use of a physical methodology to estimate the deformation of the image represented objects' shape.

In the work presented in this paper, we attend to what has already been done in the field of the physical morphing of objects, such as Nastar's analytical determination of vibration modes through the resolution of the dynamic equilibrium equation in [5-7]; Sclaorff's isoparametric finite element to model objects by the Finite Element Method (FEM) in [4, 9-11]; the and Tavares's study to match deformable objects in [12-15].

In the used approach, some of the objects' pixels (nodes) are considered already matched, and the mass and stiffness matrixes are considered determined as if the given objects were made of a virtual material.

As the dynamic equilibrium equation is solved we determine and can represent the deformations of the given objects, at each instant of time.

As we considered that no additional information was known about the given objects, or of the movement/deformation involved, to apply this physical methodology we needed the estimation of some parameters: the applied charges on matched and unmatched nodes, and the initial displacement and velocity vectors. This estimation process is also described.

With the presented work the adopted physical methodology is expanded to application cases in witch the matching isn't done successfully for all object's nodes. Another contribution of our work is the representation of the estimated morphing by the evaluated strain energy values. We also propose a image based stop criterion for the computation process: the process will stop when a estimated shape gets close enough to the target shape. As in some applications can be of interest the estimation of only the non-rigid component of the global deformation, we also adopted a solution to do this type of morphing.

In this paper will be described the FEM element applied, namely Sclaroff's isoparametric element, and the approach employed to match some objects nodes. There will also be presented an integration method that is used to solve the equilibrium equation, as well as the solutions adopted to estimate the applied charges, the initial displacement and velocity, and the procedures used to solve problems concerned with the unsuccessful matched nodes. We will also mention how global and local strain energy is evaluated, as well as the solution used to simulate only the non-rigid morphing component. Some examples of the experimental results, their respective conclusions, and future work perspectives will also be presented.

2. SCLAROFF'S ISOPARAMETRIC ELEMENT

Given a collection of sample points from an object (nodes), a set of continuous interpolation functions are built to relate the displacement of a single point to the relative displacements of all the nodes of the object. In Sclaroff's element Gaussian interpolants are used for Galerkin approximation [1, 9, 10, 12]:

$$g_i(X) = e^{-\|X - X_i\|^2/(2\sigma^2)}, \quad (1)$$

where X_i is the function's n-dimensional center, and σ its standard deviation (which controls data interaction by increasing the models' stiffness [12]). The interpolation functions, h_i, of the interpolation matrix, *H*, are given by:

$$h_i(X) = \sum_{k=1}^{m} a_{ik} g_k(X), \quad (2)$$

where a_{ik} are coefficients with value one at node i, and zero at all other nodes, and m is the number of nodes.

The interpolation coefficients a_{ik}, elements of matrix *A*, can be determined by inverting matrix G defined as:

$$G = \begin{bmatrix} g_1(x_1) & \cdots & g_1(x_m) \\ \vdots & \ddots & \vdots \\ g_m(x_1) & \cdots & g_m(x_m) \end{bmatrix}. \quad (3)$$

And by doing so the interpolation matrix of Sclaroff's isoparametric element for a 2D object will be:

$$H(X) = \begin{bmatrix} h_1 & \cdots & h_m & 0 & \cdots & 0 \\ 0 & \cdots & 0 & h_1 & \cdots & h_m \end{bmatrix}. \quad (4)$$

The mass and stiffness matrixes, M and K respectively, can then be built (see e.g. [8, 9, 10, 12, 13]).

The used damping matrix, C, was considered as a linear combination of the mass and stiffness matrixes (this type of damping is known as Rayleigh's damping):

$$C = \hat{\alpha} M + \hat{\beta} K, \quad (5)$$

where $\hat{\alpha}$ and $\hat{\beta}$ are respectively the mass and stiffness constants determined by the desired critical damping (depending on the adopted virtual material) [2].

3. MODAL MATCHING

To match the m and n nodes of the initial and target shapes, t and $t+1$ respectively, each generalized eigenvalue problem is solved:

$$K\Phi = M\Phi\Omega, \quad (6)$$

where for a 2D model with m nodes:

$$\Omega = \begin{bmatrix} \omega_1^2 & & 0 \\ & \ddots & \\ 0 & & \omega_{2m}^2 \end{bmatrix}. \quad (7)$$

and

$$\Phi = \left[\phi_1 \mid \cdots \mid \phi_{2m}\right] = \begin{bmatrix} u_1^T \\ \vdots \\ u_m^T \\ v_1^T \\ \vdots \\ v_m^T \end{bmatrix} \quad (8)$$

The shape vector of mode i, ϕ_i, describes, the displacement (u, v) of each node due to mode i, and in the diagonal matrix Ω the frequency of vibrations' squares are increasingly ordered. With the modal matrixes Φ_t and Φ_{t+1}, some nodes can be matched by comparing their displacement in the modal eigenspace. To do so, a affinity matrix, Z, is built with elements:

$$Z_{ij} = \left\|u_{1,i} - u_{2,j}\right\|^2 + \left\|v_{1,i} - v_{2,j}\right\|^2. \quad (9)$$

In this affinity matrix, the best matches are indicated by the minimum values of line and column: the affinity between nodes i and j will be null if the match is perfect and increases as the match worsens [12, 13, 14]. Usually the rigid modes and the high order modes are not considered in this building process to discard the rigid component of the deformation and to reduce the sensitivity to noise[9, 10].

This modal matching can provide good matching results between two objects if the involved deformation is not very severe. However, our morphing approach can also be used if the matching is done by another process.

4. RESOLUTION OF THE DYNAMIC EQUILIBRIUM EQUATION

In this work the physical morphing is done by solving Lagrange's Dynamic Equilibrium Equation:

$$M\ddot{U}^t + C\dot{U}^t + KU^t = R^t, \quad (10)$$

where the nodal displacements, U, in the instant of time *t*, can be described by:

$$U_i = X_{2,i} - X_{1,i}, \quad (11)$$

where $X_{1,i}$ is the i^{th} node of the initial shape and $X_{2,i}$ of the target shape, and U_i is the displacement of the i^{th} node.

To solve the above equation, several integration methods can be used. In this paper we presented the mode superposition method with Newmark´s method.

4.1 Mode Superposition Method

This integration method obtains new matrixes of stiffness, mass and damping with smaller bandwidth [1], allowing the resolution of the dynamic equilibrium equation (10) with only a part of the modes. This measure reduces the associated computational cost by ignoring the movement's local components, essentially associated to noise. With this measure, the computation is accelerated without great loss of detail [8].

This method proposes the transformation Φ used to transform the modal displacements, X, into nodal displacements, U:

$$U^t = \Phi X^t, \quad (12)$$

and therefore we can write the corresponding equilibrium equations using generalized coordinates:

$$\ddot{X}^t + \Phi^T C \Phi^t + \Omega^2 X^t = \Phi^T R^t , \quad (13)$$

where $\ddot{X}$ and $\dot{X}$ are, respectively, the first and second order derivatives of the modal displacement vector, because:

$$\Phi^T K \Phi = \Omega^2 \text{ and } \Phi^T M \Phi = I , \quad (14)$$

where I represents the identity matrix.

4.2 Newmark's Method

To solve (13), we used Newmark's method that considers:

$$\begin{cases} \dot{X}^{t+\Delta t} = \dot{X}^t + \left[(1-\delta)\ddot{X}^t + \delta \ddot{X}^{t+\Delta t} \right] \Delta t \\ X^{t+\Delta t} = X^t + \dot{X}^t \Delta t + \left[\left(\frac{1}{2} - \alpha \right) \ddot{X}^t + \alpha \ddot{X}^{t+\Delta t} \right] \Delta t^2 \end{cases} \quad (15)$$

where α and δ are determined in order to satisfactory and stable results can be obtained [1].

Replacing (15) into (13) we obtain:

$$\left(\frac{1}{\alpha \Delta t^2} I + \frac{\delta}{\alpha \Delta t} \Phi^t C \Phi + \Omega^2 \right) X^{t+\Delta t} =$$

$$= R^t + \left(\frac{1}{\alpha \Delta t^2} I + \frac{\delta}{\alpha \Delta t} \Phi^t C \Phi \right) X^t \quad . \quad (16)$$

$$+ \left(\frac{1}{\alpha \Delta t} I - \left(1 - \frac{\delta}{\alpha} \right) \Phi^t C \Phi \right) \dot{X}^t$$

$$+ \left(\frac{1-2\alpha}{2\alpha} I - \left[(1-\delta)\Delta t - \frac{1-2\alpha}{2\alpha} \Delta t \delta \right] \Phi^t C \Phi \right) \ddot{X}^t$$

According to [2], this method is unconditionally stable for $2\alpha \geq \delta \geq 0.5$. However, if $\delta = 0.5$ this method does not have numerical damping (for any value of α). If $\delta > 0.5$, then artificial damping is introduced, but the obtained results are also less accurate.

When:

$$\alpha = \frac{1}{4} \left(\delta + \frac{1}{2} \right)^2 , \quad (17)$$

the high frequency dissipation is maximized for any value of $\delta > 0.5$ [2]. In practice, we noticed that in some experimental cases the precision reduction can lead to undesired results (the results diverge from the target shape) [8].

5. ESTIMATES

In this section we will describe the solution used to solve some problems related to the lack of information about the given objects and their deformation: the estimation of the initial velocity and displacement vectors, and of the charges applied on the nodes (successfully matched or not).

5.1 Initial Displacement and Velocity

The used integration method requires the initial displacement and velocity vectors. The solution adopted to estimate the initial displacement was to consider it in terms of the expected displacement. So, the initial displacement was considered as:

$$X^0(i) = c_X (X_{2,i} - X_{1,i}) , \quad (18)$$

where $X^0(i)$ represents the i^{th} component of the modal initial displacement, and c_X is a constant to be determined by the user.

Similarly, the initial modal velocity was considered in terms of the initial modal displacement:

$$\dot{X}^0(i) = c_V X^0(i) , \quad (19)$$

where c_V is a user defined constant (in this work c_X and c_V were considered equal for all nodes).

As bigger values of c_X e c_V are chosen, the displacements also get larger, and the target shape can be obtained sooner.

5.2 Applied Charges

The applied charges on the matched nodes are supposed to be proportional to the expected nodal displacement:

$$R(i) = k(X_{2,i} - X_{j,i}) , \quad (20)$$

where $R(i)$ is the applied charges i^{th} vector component when i is a matched node, $X_{2,i}$ its coordinates in the target shape, $X_{j,i}$ its coordinates in the j^{th} shape, and k is a global stiffness constant (once again, equal for all R's components).

5.3 Unmatched Nodes

However, since not all nodes might be successfully matched (for instance by modal matching), to estimate the applied charges on the unmatched nodes we used a neighborhood criterion [8]. And so, nodes preserve their order during motion, and the unmatched nodes are attracted to the nodes between the adjacent matched nodes. For e.g. (figure 1) if B is a unmatched node between A and C (respectively matched with A' and C'), and if B is the applied charges vector i^{th} component, then:

$$R(i) = k \left(\sum_{\substack{B' \text{ all} \\ \text{nodes between} \\ A' \text{ and } C'}} \left[\frac{D_{tot} - D_{B'}}{D_{tot}} \left(X_{2,B'} - X_{1,i} \right) \right] \right) , \quad (21)$$

where D_{tot} represents the sum of the distances between all involved nodes and $D_{B'}$ is the distance between B and a unmatched node of the target shape.

However the initial displacement solution presented in (18) was not defined for unmatched nodes. So, as we had already estimated the applied charges on the unmatched nodes, we recursively specified the initial displacement in terms of the applied charges. So we considered:

$$\begin{cases} X^0(i) = \frac{c_X}{k} R(i) & \text{if } k \neq 0 \\ X^0(i) = 0 & \text{if } k = 0 \end{cases} , \quad (22)$$

and, unless k is null, the initial modal displacement of the matched nodes equals (18).

As we can see in (21), for each unmatched node of the first shape, the initial modal displacement is influenced, such as the applied charges, by the nodes of the final shape that are between the nodes that match its adjacents neighbors. And each node's weight was considered equal to the corresponding value of the applied charges vector.

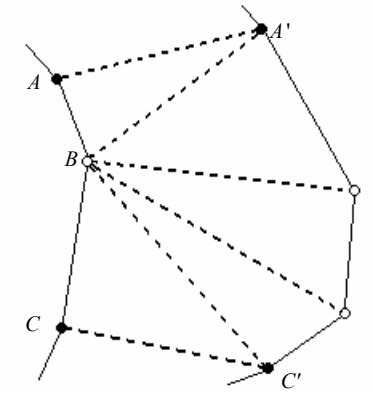

Figure 1: Used criterion to estimate the applied charges on the unmatched node *B* (*A* is matched with *A'* and *C* with *C'*).

6. OTHER RESULTS

In this section we present two extensions of this methodology that can be useful. First we describe how strain energy can be evaluated, and second we describe how morphing can be done by considering only the non-rigid components.

6.1 Strain Energy

The involved strain energy, E, was evaluated in this work by:

$$E = U^T K U \ . \tag{23}$$

So if:

$$U = \begin{pmatrix} u_1 \\ u_2 \\ \vdots \\ u_n \end{pmatrix}, \text{ and } K = \begin{pmatrix} k_{11} & k_{12} & \cdots & k_{1n} \\ k_{21} & k_{22} & \cdots & k_{2n} \\ \vdots & \vdots & \ddots & \vdots \\ k_{n1} & k_{n2} & \cdots & k_{nn} \end{pmatrix}, \tag{24}$$

then:

$$E = \sum_{i=1}^{n} u_i \sum_{j=1}^{n} k_{ij} u_j \ . \tag{25}$$

As we can see in the last equation, the global strain energy is the result of the sum of its local components, which means that the strain energy associated to the i^{th} node, e_i, is:

$$e_i = u_i \sum_{j=1}^{n} k_{ij} u_j \ . \tag{26}$$

Therefore, once the displacement field between the given objects is determined, one can represent the intermediate shapes according to the global or local strain energy levels (figures 2 and 3 – where lighter levels of grey represent higher energy).

6.2 Only Non-Rigid Morphing

It may be of some application areas'interest the estimation of only the non-rigid components of the deformation involved. To do so the rigid transformation component can be applied to the first shape, and the obtained shape is considered as the new initial shape. The rigid transformation component applied in this work is composed by a rotation about the origin, a scale about the same point, and finally a translation [3, 12]. Then, a new shape is obtained and the resolution of the dynamic equilibrium equation proceeds as described (figures 4 and 5).

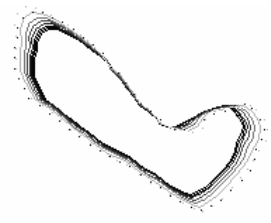

Figure 2: Results obtained from two contours of real pedobarography images represented according to global strain energy levels.

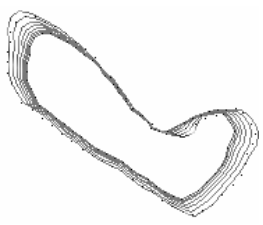

Figure 3: ... according to local strain energy levels.

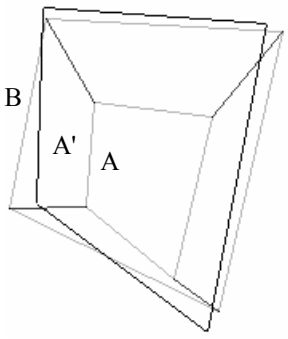

Figure 4: Modal matching between contours A and B, and the result, A', of the applied rigid transformation estimated to the initial contour.

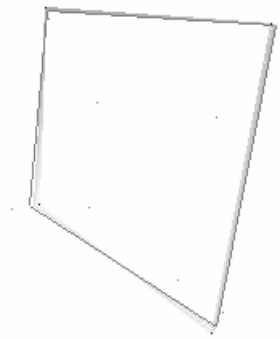

Figure 5: Only the non-rigid component of morphing between A and B is obtained.

7. EXPERIMENTAL RESULTS

This methodology was implemented in a platform to develop and test image processing and analysis, and computer graphics algorithms (for a detailed presentation see [15]). This section presents some of the obtained experimental results.

We used the proposed methodology with contour objects because the behavior of 2D objects can almost always be simulated using only its contour without a critical loss of information and with a reduced computational cost (although this methodology also works with inner points).

Notice that all presented images include the nodes of the initial and target shapes, and the obtained results are in grey scale according to the applied charges, or to the global or local strain energy values (all nodes of the same intermediate shape are linked by line segments). Also, lower levels of charges or energy are represented with darker tones of grey.

For the fist experience, consider contours C and D represented in figure 6. When polyethylene is used as a virtual material, the global stiffness constant $k = 1$, the time step $\Delta t = 1$, critical damping levels are between 0.5% and 3%, the mode superposition method with Newmark's method uses 7 steps (figures 7 and 8 are represented in values of local and global strain energy, respectively). In any of the mentioned figures we are able to notice that there is an increase on the stain energy values due to the increasing displacement between steps (figure 9). However, if the approach criterion is not used, the method will only stop if the forces equilibrium is achieved, consequently the number of used steps will be bigger, the displacements between steps decrease, and the strain energy values will decrease. Instead, the approach criterion allows the procedure to stop before equilibrium is achieved, and so the results presented can get better, but with a considerable increase of the number of steps used. As the estimated shapes approach the target shape, the applied charges' intensities decrease. So, in the process limit, the approach stop criterion can be equivalent to the forces equilibrium criterion.

In resume, with the proposed stop criterion reasonable approaches can be obtained quicker, and it is easier to control (because it is more comfortable to specify a distance in pixels than with a force's value).

Considering now the contours E and F (figure 10), with 47 of their 57 nodes successfully matched, in figure 11 and 12 we can notice that the values of the global stiffness constant can also control the approach to the target shape, since higher intensities of the applied charges can take to quicker convergence (with the constraints established by the virtual material used - beyond those

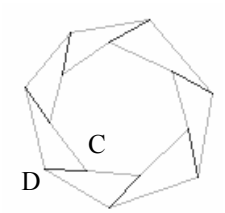

Figure 6: Modal matching between contours C and D.

Figure 7: Intermediate shapes according to local strain energy values.

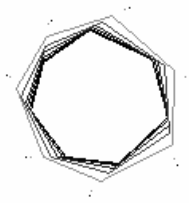

Figure 8: ... to global strain energy values.

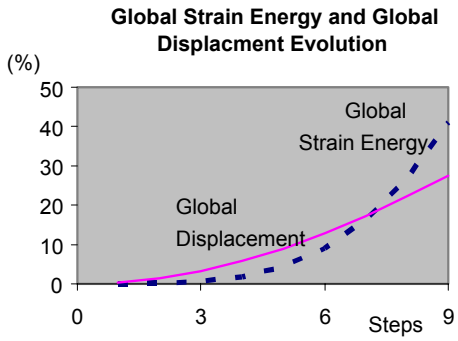

Figure 9: Global strain energy and displacement evolution during morphing in figure 9.

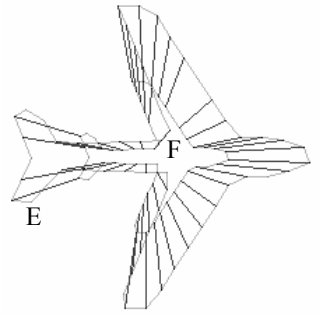

Figure 10: Modal matching between contours E and F.

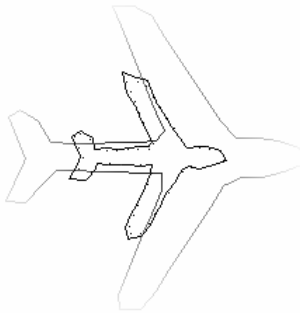

Figure 11: Initial and final shapes according to applied charges intensities when $k = 60$.

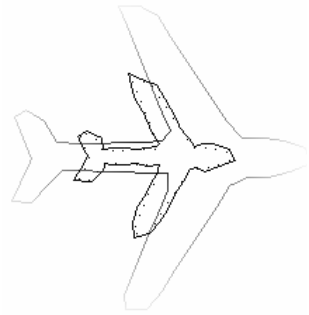

Figure 12: ... $k = 30$.

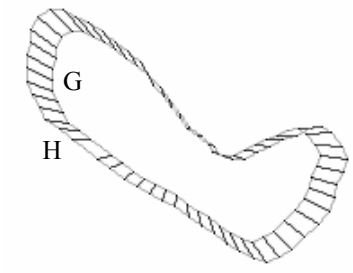

Figure 13: Modal matching between contours G and H.

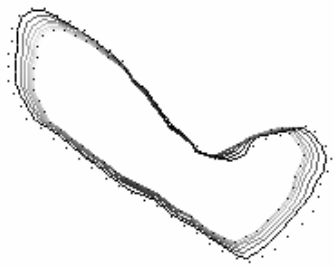

Figure 14: Intermediate shapes according to applied charges intensities when all modes are considered.

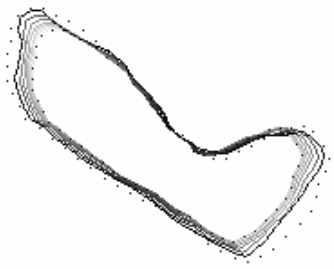

Figure 15: …when 2/3 modes are considered.

values results will diverge).

For the last experience, consider contours G and H, represented in figure 13, with 61 nodes (each) of which 59 are successfully matched. Under the mentioned conditions for examples C and D, with a stop criterion based on the approach to the target shape at less than 220 pixels (which is equivalent to a medium approach of each node below than 3.7 pixels) the mode superposition method, solved with the Newmark's method, using all modes needs 8 steps, while with 2/3 of the modes 10 steps are needed (figures 14 and 15). If less modes are used the computational cost will decrease, but generally the results' precision will also be lost.

8. CONCLUSIONS AND FUTURE WORK

This paper presents a methodology to do physics based morphing between image represented objects.

If all nodes of the given shapes are matched, then the applied charges are considered as proportional to the distances between each node and its pair. This solution can't be adopted for the unmatched nodes, because we don't know each node's pair. To overcome this application restriction, we adopted a solution based on the neighborhood criterion. With this solution, reasonable approaches of the target shape can be obtained even when the number of unmatched nodes is significant.

The intermediate shapes estimated, by the proposed methodology, can be represented according to the intensities of the applied charges, or of the global or local strain energy. Those values can be estimated in each integration step because this methodology is based on physical principles.

In this paper, a solution is also presented to simulate only the non-rigid morphing, which might be of interest to some of this methodology's application domains. When the rigid transformation is applied ahead of the resolution of the equilibrium equation, as expected, the number of used steps is lower and displacements between steps are smaller.

In this paper the dynamic equilibrium equation has been solved using the mode superposition method with Newmark's method. We noticed that when only a part of the modes are used, the computational effort is reduced, but there is a decrease on accuracy.

In future this approach should be expanded to 3D objects, since we have only worked with 2D data until now.

To estimate the applied charges we used in this work fixed global stiffness constants and fixed time steps, but physical morphing can also be done in a way that, in each integration step, more information is added to the resolution process, allowing the constants variability.

Another future task is the necessary validation of proposed methodology with real application examples. For instance, in the domain of computer graphics this methodology may be used to simulate the collision between objects; or in medical image it can be used to reconstruct intermediate images when two images are given.

9. REFERENCES

[1] Bathe, K., Finite Element Procedures, Prentice-Hall, 1996

[2] Cook, R., Malkus, D., Plesha, M., Concepts and Applications of Finite Element Analysis, Wiley, 1989

[3] Horn, B., Closed-Form Solution of Absolute Orientation using Unit Quaternions, Journal of the Optical Society America A., 1987

[4] Martin, J., Pentland A., Sclaroff, S., Kikinis, R., Characterization of Neuropathological Shape Deformations, IEEE Transactions on Pattern Analysis and Machine Intelligence, vol. 20, no. 2, Feb. 1998

[5] Nastar, C., Ayache, N., Fast Segmentation, Tracking, and Analysis of Deformable Objects, Fourth International Conference on Computer Vision, Berlin, Germany, 1993

[6] Nastar, C., Modèles Phisiques Déformables et Modes Vibratoires pour l'Analyse du Mouvement non-rigide dans les Images Multidimensionnelles, L'École Nationale des Ponts et Chaussées, 1994

[7] Nastar, C., Ayache, N., Frequency-Based Nonrigid Motion Analysis: Application to Four Dimensional Medical Images, IEEE Transactions on Pattern Analysis and Machine Intelligence, vol. 18, 1996

[8] Pinho, R., Determinação do Campo de Deslocamentos a partir de Imagens de Objectos Deformáveis, Universidade do Porto, 2002

[9] Sclaroff, S., Modal Matching: A Method for Describing, Comparing, and Manipulating Digital Signals, MIT, 1995

[10] Sclaroff, S., Pentland, A., Modal Matching for Correspondence and Recognition, IEEE Transactions on Pattern Analysis and Machine Intelligence, June, 1995

[11] Sclaroff, S., Deformable Prototypes for Encoding Shape Categories in Image Databases, Pattern Recognition, vol. 30, no. 4, pp. 627-642, Apr. 1997

[12] Tavares, J., Análise de Movimento de Corpos Deformáveis usando Visão Computacional, FEUP, 2000

[13] Tavares, J., Barbosa, J., Padilha, A., Determinação de Correspondência entre Modelos de Contorno e de Superfície, utilizando Modelização por Elementos Finitos e Análise Modal, em Visão por Computador, VI Congresso Nacional de Mecânica Aplicada e Computacional, Aveiro, 2000

[14] Tavares, J., Barbosa, J., Padilha, A., Matching Image Objects in Dynamic Pedobarography, RecPad'2000 11th Portuguese Conference on Pattern Recognition. Porto, Portugal, 2000

[15] Tavares, J., Barbosa, J., Padilha, A., Apresentação de um Banco de Desenvolvimento e Ensaio para Objectos Deformáveis, RESI - Revista Electrónica de Sistemas de Informação, vol. 1, 2002